Hough Transform and Laguerre Geometry for the Recognition and Reconstruction of Special 3D Shapes

M. Peternell, H. Pottmann, T. Steiner
Institute of Geometry, Vienna University of Technology,
Vienna, Austria

September 5, 2003

Abstract

We put the Hough transform, a method from Image Processing, into relation to Laguerre geometry, a concept of classical geometry, and study both concepts in the 3D case. It is shown how Laguerre geometry, which works in the set of oriented planes, is used in the detection of special shapes such as planes, spheres, rotational cones and cylinders, general cones and cylinders, and general developable surfaces. We perform shape recognition tasks by principal component analysis on a set of points in the so-called Blaschke model of Laguerre geometry. These points are Blaschke image points of estimated tangent planes at the given data points. Finally we present examples and show how the implementation also takes advantage of mathematical morphology on images, which are defined on meshes.

1 Introduction

The recognition and reconstruction of 3D shapes from 3D measurement data is an important issue in various applications. These include reverse engineering of CAD models from existing technical objects [28], the reconstruction of 3D city models from airborne laser scanner data [30] or as-built reconstructions of industrial sites such as oil platforms, plants and refineries [14]. In

these applications it is essential that special shapes such as planes, spheres, cylinders, etc., are not just fitted by a freeform surface, but represented in a more precise way according to their simple geometric nature.

In the present paper, we deal with the problem of *recognizing and reconstructing special 3D shapes* from 3D data. This may be a cloud of measurement points or another 3D shape representation such as a triangular mesh or a surface representation in parametric or implicit form. The only assumption we make is that we are able to compute a discrete number of points on the surface and to estimate surface normals there. The availability of normals is not necessary for some considerations, but is not a heavy restriction, especially since recent scanners also deliver the normal information.

We are dealing with the following special surfaces: planes, spheres, cones and cylinders, in particular those with rotational symmetry, and general developable surfaces.

1.1 Review of previous work

Let us briefly address the main approaches to the present problem.

In Computer Vision, Image Processing and Pattern Recognition, the detection and reconstruction of special shapes is often performed by methods related to the *Hough transform*. Originally designed for the detection of straight lines in 2D images, it received an enormous amount of attention and has been generalized to the detection and reconstruction of many other shapes (see, e.g., the survey articles [9, 10]). Pure Hough transform methods work in the space of considered shapes. Therefore, they quickly lead to high dimensions and thus to reduced efficiency.

To reduce the dimension of the search space, Hough transform techniques are sometimes mixed with constructive geometric considerations [9]. Those approaches are already close to techniques invented by the CAD community. In this community geometric properties of surfaces, which are mainly based on the *Gaussian sphere*, are used to segment the data and to extract special shapes, see [27, 28].

Methods based on *line geometry* [20] recognize cylinders, surfaces of revolution and helical surfaces by the fact that their normals lie in a so-called linear line complex. Thus, one fits a linear complex to estimated normals at the data points, which is an eigenvalue problem. In particular, surfaces which allow multiple self-motions, namely right circular cylinders, spheres and planes are detected from the distribution of eigenvalues. Moreover, the

technique is extendable to other surface classes which may be locally well approximated by the mentioned surface types [3, 20].

Another class of methods uses locally estimated tangent planes at the data points and thus operates in the *space of planes*. Projective duality makes it easy to handle projective and algebraic properties. Especially for developable surfaces this has been pursued successfully [20]. Moreover, after removing all planes, which are parallel to some selected line, one can introduce a metric in the space of remaining planes and solve approximation problems there. This has also been used for surface recognition and reconstruction [16, 19].

1.2 Contributions of the present paper

In the present paper, we also work in the set of planes in $\mathbb{R}^3$. However, we do not use projective duality, since it has the disadvantage that approximation aspects require the removal of planes which might be in the area of interest. What we are proposing here is an extension of the Gaussian sphere, which is rooted both in classical *Laguerre geometry* [1, 2, 4] and in the Hough transform method [9, 10]. Applications of Laguerre geometry in CAGD, in particular from the algebraic viewpoint and its relation to offsets, have been given in several contributions [17, 18]. Although we do not use Laguerre transformations as an invariance group and thus the techniques are not belonging to Laguerre geometry in its strict sense, there is still a big advantage to use the classical knowledge in the present setting.

The Gaussian image of an oriented plane in $\mathbb{R}^3$ with unit normal vector $\mathbf{n}$ is the point $\mathbf{n}$ on the unit sphere $S^2 \subset \mathbb{R}^3$. The Gaussian preimages of a point $\mathbf{n} \in S^2$ are parallel planes with equation $\mathbf{n} \cdot \mathbf{x} + d = 0$. The distance d of the origin to the plane is neglected by the Gaussian image. However, the Blaschke model of Laguerre geometry uses this distance and considers as image point of the plane the point $(\mathbf{n}, d) \in \mathbb{R}^4$. Thus, the image points of all oriented planes fulfill the so-called *Blaschke cylinder* $B : \mathbf{n}^2 = 1$ in $\mathbb{R}^4$. Its cross sections are copies of the Gaussian sphere S^2.

In the present paper, we present elementary derivations of a number of remarkable properties of this cylinder model, which are interesting for the present application. They allow us to use fitting by hyperplanes (principal component analysis) in the recognition and reconstruction procedure. The distribution of eigenvalues (principal components) gives information on special shapes such as spheres, cones and cylinders, in particular those with rotational symmetry. Moreover, developable surfaces can be recognized and

classified in a simple way, and important information about their reconstruction is derived as well.

An appropriate discretization of the Gaussian sphere and the Blaschke cylinder is used in the implementation. It turns out that techniques from *mathematical morphology* [7, 24, 25] are very useful for the implementation of the proposed methods. However, there are just very few contributions [8, 12, 21, 22, 29] which extend morphology to curved manifolds and to meshes and cell decompositions on curved manifolds, such as the Blaschke cylinder. We also present initial results on this topic and outline directions for future research which are related to the present shape recognition and reconstruction problem.

The paper is organized as follows. In section 2 we briefly describe the classical 2D Hough transform and relate it to the Blaschke cylinder of 2D Laguerre geometry. Section 3 presents 3D Laguerre geometry, a discretization of the Blaschke cylinder and a corresponding Hough transform for the detection of planes in $\mathbb{R}^3$. Section 4 further elaborates on the Blaschke model and uses it for surface recognition. Implementation issues, mathematical morphology and examples are presented in section 5. We conclude with an outlook to future research.

2 Hough transform for lines in the plane and the Blaschke model of 2D Laguerre geometry

Using Cartesian coordinates $(x, y) =: \mathbf{x}$, a straight line L in the Euclidean plane can be written in the Hesse normal form,

$$n_1 x + n_2 y + d = 0, \quad n_1^2 + n_2^2 = 1. \tag{1}$$

Recall that $n_1 x + n_2 y + d$ is the signed distance of the point (x, y) to L. In particular, d is the (signed) distance of the origin to L. We can parameterize the unit normal vector $\mathbf{n} = (n_1, n_2)$ with help of its directional angle ϕ, $\mathbf{n} = (\cos\phi, \sin\phi)$ and map the line L to the point $h(L) := (\phi, d)$ of another plane, called *Hough plane*. If we exclude negative values of d, we have to use $\phi \in [0, 2\pi)$. Hence, the line–to–point mapping h maps lines of R^2 to points in $[0, 2\pi] \times \mathbb{R}^+$. For practical applications, we can bound d by some constant D, such that the image lines $h(L)$ will fall into the rectangle $[0, 2\pi] \times [0, D]$.

However, we have to note that $\phi = 0$ and $\phi = 2\pi$ have to be identified, such that the topology is that of a cylinder.

Let us now consider a fixed point $\mathbf{p} = (p_1, p_2)$ and all lines L which pass through this point. The incidence condition between $\mathbf{p}$ and L is

$$p_1 \cos\phi + p_2 \sin\phi + d = 0, \tag{2}$$

and therefore the image points $h(L) = (\phi, d)$ in the Hough plane lie on the sine curve $d = -p_1 \cos\phi - p_2 \sin\phi$; of course, one takes just positive d to be consistent with the given range of d. We call the curve the Hough image $h(\mathbf{p})$ of the point $\mathbf{p}$. Given k points $\mathbf{p}_1, \ldots, \mathbf{p}_k$, which are all incident with some line G, the Hough image curves $h(\mathbf{p}_i)$ of these points must pass through the point $h(G)$. This simple observation is the basis of the *Hough transform*, whose implementation proceeds as follows.

One puts a regular grid over the Hough plane, i.e. views it at as pixel plane. Initially, all pixels have value 0. For each point $\mathbf{p}_i$, the Hough image curve $h(\mathbf{p}_i)$ is also discretized; those pixels which are met by the exact curve $h(\mathbf{p}_i)$ get a 'vote' from $\mathbf{p}_i$, i.e., their value is increased by 1. The peaks in this accumulator array now indicate nearly collinear arrangements of points in the original plane. There is a large body of literature dealing with efficient implementations and accuracy issues of this method [9, 10].

Planar Laguerre geometry [1, 2, 4] studies the set of oriented lines and the set of 'cycles', which are the oriented circles and the points, seen as circles of radius 0. In a natural way it defines the tangency between a cycle and an oriented line and studies properties which are invariant under so-called Laguerre transformations. These maps are bijective on the set of oriented lines, bijective on the set of cycles, and they keep tangency.

Laguerre geometry is studied in various models. One of these models is very closely related to the Hough plane. We have already observed, that the topology of the Hough plane is that of a cylinder. Laguerre geometry uses the cylinder: With help of a unit normal vector $\mathbf{n} = (n_1, n_2)$ a line $L \in \mathbb{R}^2$ is assigned an orientation, and it is mapped onto the point $b(L) = (n_1, n_2, d) \in \mathbb{R}^3$. In order to carefully distinguish between the original plane and the image space $\mathbb{R}^3$, we denote Cartesian coordinates in the image space $\mathbb{R}^3$ as (u_1, u_2, u_3). Under the *Blaschke mapping* b, the set of all oriented lines of $\mathbb{R}^2$ is mapped to the entire point set of the right circular cylinder B, called *Blaschke cylinder*

$$B: \; u_1^2 + u_2^2 = 1. \tag{3}$$

This equation expresses the normalization condition $\mathbf{n}^2 = 1$ of a normal vector $\mathbf{n}$ of a line L. If we omit the orientation of lines, we can use just the upper half of the cylinder B. Cutting this cylindrical part along a ruling and unfolding it into the plane yields the Hough plane.

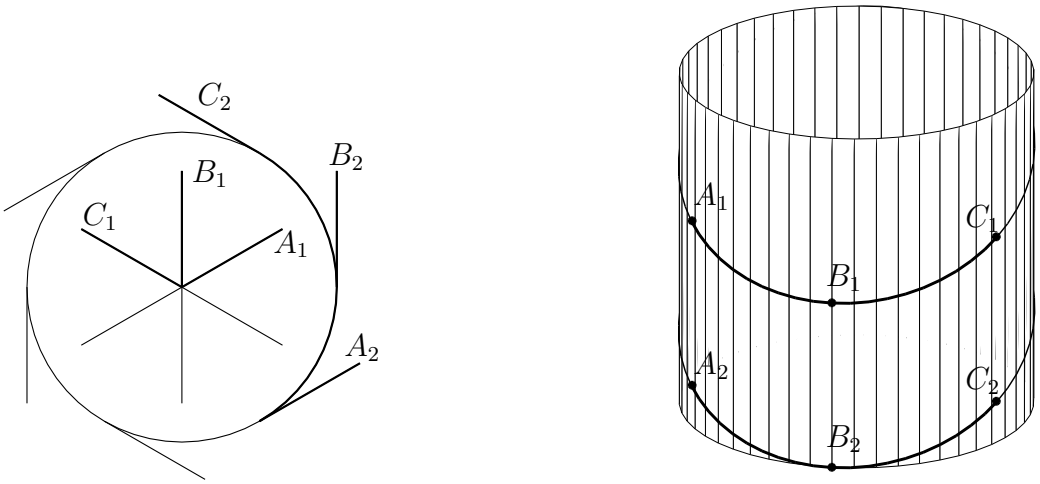

Figure 1: Blaschke images of a pencil of lines and of lines tangent to an or. circle.

Let us derive a few simple properties of the Blaschke model. The Blaschke image points $b(L)$ of all oriented lines L, which pass through a point $\mathbf{p} = (p_1, p_2)$, satisfy in view of (2) the equation

$$p_1 u_1 + p_2 u_2 + u_3 = 0. \tag{4}$$

This is a plane through the origin of $\mathbb{R}^3$. It cuts the cylinder B in an ellipse. The Blaschke image points $b(L)$ of lines L through $\mathbf{p}$ are exactly the points of this ellipse, see Fig. 1.

A point $\mathbf{p}$ is a circle of radius 0. Let us now consider all oriented lines L tangent to an oriented circle with center $\mathbf{p}$ and (signed) radius r. These tangents are exactly those oriented lines, whose signed distance from $\mathbf{p}$ equals r. Therefore, they satisfy

$$\mathbf{n} \cdot \mathbf{p} + d = r. \tag{5}$$

Their Blaschke image points are thus confined not only to B, but also to the plane

$$p_1 u_1 + p_2 u_2 + u_3 - r = 0, \tag{6}$$

and thus they lie on the intersection of this plane with B, which is an ellipse. This is also clear from the fact that passing from the circle of radius 0 to its offset at distance r implies a translation of $b(L)$ by the vector $(0, 0, r)$ in the Blaschke image, see Fig. 1.

Summarizing we can say: The oriented tangents of a cycle are in one-to-one correspondence with the curved planar intersections of B. An intersection of B with a plane H (not parallel to the u_3-axis),

$$H: \ a_0 + a_1 u_1 + a_2 u_2 + u_3 = 0,$$

is the Blaschke image of the oriented tangents of a circle with center (a_1, a_2) and radius $-a_0$; the latter can be zero.

Laguerre geometry shows that *Laguerre transformations* are seen in the Blaschke model as restrictions of those projective maps to B, which map B (as a whole) onto itself. Let us mention some simple special cases. Rotations about the origin of $\mathbb{R}^2$ are transformed with b to rotations of B about the u_3-axis. Translations $\mathbf{x}' = \mathbf{x} - \mathbf{t}$ in $\mathbb{R}^2$ are transformed to affine shear transformations in u_3 direction, $(u_1', u_2', u_3') = (u_1, u_2, t_1 u_1 + t_2 u_2 + u_3)$. A *dilation*, which maps each oriented line L, with $b(L) = (n_1, n_2, d)$, onto a parallel line L' at oriented distance c, is seen as a translation by the vector $(0, 0, c)$, since $b(L') = (n_1, n_2, d + c)$. If we view a general curve as set of its oriented tangents, this dilation maps it onto its signed offset at distance c. The fact, that offsetting is so simply represented in Laguerre geometry, makes it an attractive tool for studying offsets. For example, rational curves with rational offsets belong to (arbitrary) rational curves on B.

A Euclidean metric in the set of lines

Any Euclidean metric, which we may use in $\mathbb{R}^3$, does not have a meaning for planar Laguerre geometry; automorphic projective maps of B are not compatible with it. However, we do not aim at full Laguerre invariance, but at the use of the concept for data analysis and fitting. Hence, we require the introduction of a *metric in the set of lines of* $\mathbb{R}^2$.

We will now illustrate that the simplest choice within our framework, namely the canonical Euclidean metric in the surrounding space $\mathbb{R}^3$ of the Blaschke cylinder B, is a quite useful metric. Thus, the *distance* $d(L, G)$ *between two lines* L, G is defined to be the *Euclidean distance of their image points* $b(L)$ *and* $b(G)$.

For visualization, let us fix a line M in $\mathbb{R}^2$ as $x-m=0$. Its Blaschke image is $b(M)=(1,0,-m)$. All points of the Blaschke cylinder, whose Euclidean distance to $b(M)$ equals r, form the intersection curve s of B with the sphere $(u_1-1)^2+u_2^2+(u_3+m)^2=r^2$. This is an algebraic curve of order 4. Its points are Blaschke images $B(L)$ of lines L in $\mathbb{R}^2$, which satisfy

$$(n_1-1)^2+n_2^2+(d+m)^2-r^2=0. \tag{7}$$

Because (n_1,n_2,d) are coefficients in the linear equation of L, they are related to the general homogeneous coordinates (g_1,g_2,g_3) of that line $L:\ g_1x+g_2y+g_3=0$ by

$$n_1=\frac{g_1}{\sqrt{g_1^2+g_2^2}}, n_2=\frac{g_2}{\sqrt{g_1^2+g_2^2}}, d=\frac{g_3}{\sqrt{g_1^2+g_2^2}}.$$

We plug this into (7) and obtain the following quartic homogeneous relation in line coordinates,

$$[(2-r^2+m^2)(g_1^2+g_2^2)+g_3^2]^2=4(g_1-mg_3)^2(g_1^2+g_2^2). \tag{8}$$

Hence, all lines L, which have constant distance $d(L,M)=r$ to a fixed line M, form the tangents of an algebraic curve of class 4 (and order ≤ 8). These curves can be identified as so-called 'hypercycles', which have been introduced and studied by W. Blaschke [2]. For our applications, they bound *tolerance regions for lines* (see Fig. 2). If a line L deviates from a line M in the sense, that $b(L)$ and $b(M)$ have at most distance r, then the line L lies in a region of $\mathbb{R}^2$, which is bounded by the curve (8). Figure 2 shows the boundary curves of tolerance regions of lines $M_i: x=m_i$, for $m_i=0, 1.25, 2.5$ and radius $r=0.25$. The lines M_i are drawn dashed. The extremal perpendicular distance of lines L and M_i within the tolerance regions is r. The extremal turning angle of L against M_i is indicated by the asymptotic lines of the boundary curves, which are displayed in dotted style. For $m_i=0$, the intersection point of the asymptotic lines is at M_0, but for increasing values of $|m|$ this does not hold in general and the tolerance regions will become asymmetrically. For large values of $|m|$ this intersection point might even be outside the region, and the canonical Euclidean metric in $\mathbb{R}^3$ is then no longer useful to define distances between lines.

Note that the introduced metric is not invariant under all Euclidean motions of the plane. Rotating M about the origin, the tolerance region at distance r is undergoing the same rotation. However, for translations this is not true in view of the remarks above. If we change the distance of M

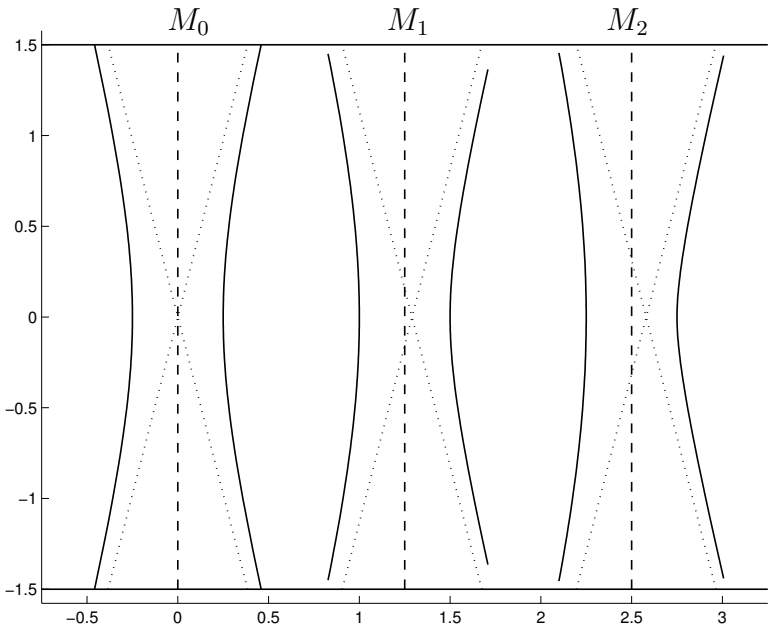

Figure 2: Boundary curves of regions containing lines having constant distance to the center lines M_i.

to the origin, then the shape of the tolerance region also changes. However, Fig. 2 shows that within some circular area of interest around the origin, the change is not dramatic and thus the introduced metric is still useful. For applications, we will therefore place the origin in the center of the data set to be analyzed and we scale the data uniformly in a way that the coordinates are < 1.

Metric considerations are also important when one discretizes a Hough image space. The cells should belong to useful tolerance regions of the analyzed shapes in object space. However, a closer inspection of the literature on Hough tranforms shows that this aspect has not received too much attention so far.

3 Hough transform for planes and the Blaschke model of 3D Laguerre geometry

3.1 Shape recognition using the Gaussian sphere

Consider a smooth oriented surface Φ in $\mathbb{R}^3$. The orientation is given by a field of unit normal vectors $\mathbf{n}$ of Φ. For applications, where Φ is the boundary of a solid S, the orientation can be chosen such that the normals point to the exterior of S. The Gaussian mapping γ maps points of Φ to the unit sphere S^2: a point $\mathbf{x} \in \Phi$, with unit normal vector $\mathbf{n}$ to Φ, is mapped to the point $\mathbf{n} \in S^2$.

It is known that the Gaussian image of an *oriented plane* Φ is just a single *point*.

A *general cylinder surface* $\mathbf{x}(u, v) = \mathbf{l}(u)+v\mathbf{r}$ is formed by a smooth family of parallel straight lines (direction vector $\mathbf{r}$), called rulings or generators. All normal vectors $\mathbf{n}$ of a cylinder are orthogonal to the rulings, and thus the Gaussian image is a *great circle* in a plane with normal vector $\mathbf{r}$.

A *right circular cone* has normals $\mathbf{n}$, which form a constant angle ϕ with its axis (direction vector $\mathbf{a}$). Hence, its Gaussian image is a *small circle*, whose axis is given by $\mathbf{a}$. A *general, non-rotational cone*, formed by lines through a fixed point, has a *nonplanar curve* as Gaussian image.

A *developable surface* Φ is a surface which can be mapped isometrically into the plane. Because of this property, these surfaces play an important role in various applications, for example in sheet metal and plate metal based industry. Assuming sufficient differentiability, developable surfaces are characterized by vanishing Gaussian curvature K. This implies that the Gaussian image is a *curve*. Clearly, all surfaces discussed in this section are developable. The remaining type of developable surfaces are those, which are formed by the tangents of a space curve. Thus, all developable surfaces are ruled, but the converse is not true. Only those ruled surfaces, which possess a constant tangent plane along each ruling are developable, and exactly because of this property, $\gamma(\Phi)$ is a curve.

The Gaussian image is used as a shape detection method for reverse engineering [28]: One estimates normals at the given data points and investigates their image on the Gaussian sphere. Planar surfaces give rise to point-like clusters on S^2, other developable surfaces generate curve-like clusters, with special cases as outlined above. However, there are several disadvantages

including the following ones.

- A translation does not effect the Gaussian image. Parallel planes, coaxial cylinders, offset pairs of cones, etc., cannot be separated by the Gaussian image.
- Not only right circular cones have a small circle as Gaussian image, all developable surfaces of constant slope have the same property. Analogously, from a great circle on S^2, one cannot conclude on a right circular cylinder.
- The γ-image of a solid, which is not just bounded by developable surfaces, covers the entire Gaussian sphere, partially in multiple ways.

All these disadvantages basically arise from the fact, that the Gaussian image is a 2-dimensional image of the 3-dimensional set of oriented planes in $\mathbb{R}^3$, and thus it eliminates one dimension.

3.2 The Blaschke model for oriented planes in 3-space

Given our derivations above, the reader may immediately realize how to overcome the problem. We build up the Blaschke model of the set of oriented planes in $\mathbb{R}^3$ in an analogous way as we have done it for lines in the plane. This model does not suffer from a loss of dimension and we show that it serves well for our purpose.

We can be brief with the Blaschke model of the set of planes of $\mathbb{R}^3$ itself, since the generalization from 2D to 3D is straightforward:

An oriented plane P in $\mathbb{R}^3$ with unit normal vector $\mathbf{n} = (n_1, n_2, n_3)$ is represented as

$$n_1 x + n_2 y + n_3 z + d = 0, \quad n_1^2 + n_2^2 + n_3^2 = 1. \tag{9}$$

We map it to the point $b(P) = (n_1, n_2, n_3, d) \in \mathbb{R}^4$. This Blaschke image point lies on the Blaschke cylinder

$$B: \; u_1^2 + u_2^2 + u_3^2 = 1. \tag{10}$$

The base surface of B in $u_4 = 0$ is exactly the Gaussian sphere. Obviously, the Blaschke image is nothing else than a graph of the support function, which plots the distance d to the origin over the Gaussian image point $\mathbf{n}$.

All oriented planes P, which are tangent to an oriented sphere with center $\mathbf{p}$ and (signed) radius r, have signed distance r from $\mathbf{p}$. Therefore, they satisfy

$$\mathbf{n} \cdot \mathbf{p} + d = r. \tag{11}$$

Their Blaschke image points lie in B and in the hyperplane (3-dimensional affine space)

$$p_1 u_1 + p_2 u_2 + p_3 u_3 + u_4 - r = 0. \tag{12}$$

Thus, the Blaschke image points form an ellipsoid on B.

Conversely, any cut of B with some hyperplane H, which is not parallel to the u_4-axis,

$$H: \; a_0 + a_1 u_1 + a_2 u_2 + a_3 u_3 + u_4 = 0,$$

is the Blaschke image of the oriented tangent planes of an oriented sphere with center (a_1, a_2, a_3) and radius $-a_0$. In particular, if $a_0 = 0$, we get oriented planes through the point (a_1, a_2, a_3).

Everything we have said about Laguerre transformations and metric considerations carries over to 3D in a straightforward way. The tolerance zone of an oriented plane M is rotationally symmetric with respect to the normal n from the origin onto M. In the planes through n we have the 2D case, and thus the 2D case has been sufficient for visualization. It also justifies the definition of a metric in the space of oriented planes in $\mathbb{R}^3$ via the canonical Euclidean distance in $\mathbb{R}^4$.

3.3 Discretization of the Blaschke cylinder for a 3D Hough transform

The Blaschke cylinder B is the Cartesian product of the unit sphere S^2 and the real line $\mathbb{R}$. An appropriate discretization of B is given by the Cartesian product of a discretized sphere and a discretized real line. The latter is trivial: assuming origin distances $|d| \leq D$, we regularly divide the interval $[-D, D]$ into $2N$ intervals of length $l = D/N$. A discretization of S^2 can be based on so-called *geodesic spheres*. These are polyhedra with vertices on S^2, which are obtained via subdivision from a regular icosahedron.

One variant splits each triangle via edge midpoint insertion into 4 triangles and then displaces the inserted edge midpoints radially onto S^2. In the first step, this yields a polyhedral approximation of S^2 with $20 \cdot 4$ faces.

Iterative application of the same procedure gives in depth k a polyhedron S_k with $20 \cdot 4^k$ triangular faces. The triangles are not regular, but close to regular, see Figures 4 and 5.

The cells of the discretized Blaschke cylinder should be close to spherical for the use in a Hough transform, since we compute distances in the Blaschke model with the canonical Euclidean metric in $\mathbb{R}^4$. To achieve this, the interval length l can be chosen as the average edge length of S_k's triangular faces.

A *Hough transform* for the *detection of nearly coplanar arrangements in a set of data points* $\mathbf{p}_1, \ldots, \mathbf{p}_k$ proceeds as follows. We place the origin in the barycenter of the data points and call the new coordinate vectors again $\mathbf{p}_i$. Moreover, we use a discretization B_d of the Blaschke cylinder and set the values in all cells equal to zero. Each point $\mathbf{p}_i = (p_{i,1}, p_{i,2}, p_{i,3})$ is viewed as bundle of incident planes and thus gives rise to a hyperplane $H_i : p_{i,1}u_1 + p_{i,2}u_2 + p_{i,3}u_3 + u_4 = 0$ in $\mathbb{R}^4$. The values of those cells in B_d, which are met by H_i are increased by one. At the end, the centers of the cells with the highest scores are Blaschke images of planes which are close to 'many' data points. Clearly, one will then compute a regression plane to those data points.

Dealing with oriented planes is not necessary here. We can confine the considerations to planes with $d \in [0, D]$.

An efficient implementation has to use several techniques which have been invented in the standard case. Surprisingly, we did not find exactly the presented version of a Hough transform for planes in the literature. Muller and Mohr [13] parameterize S^2 with longitude ϕ and latitude θ and in this way map it to a rectangle; this yields heavy distortions near the poles of the parameterization. Vosselman and Dijkman [30] pursue the approach suggested by projective geometry: they eliminate planes parallel to some line, say the z-axis, write them as $z = ax + by + c$ and map them to points (a, b, c). This is suitable for their application, but not for a general concept.

4 Recognition of special surfaces with help of the Blaschke model

4.1 Special surfaces and their Blaschke image

Right circular cone and cylinder

Consider two oriented spheres C_0, C_1 with different centers $\mathbf{m}_0, \mathbf{m}_1$ and radii r_0, r_1. The signs of the radii are chosen in a way that there exists a family of common oriented tangent planes of C_0 and C_1. The radii r_0, r_1 could be equal. These tangent planes T envelope a *cone or cylinder of revolution* Φ, with an axis spanned by $\mathbf{m}_0, \mathbf{m}_1$. According to equation (12), the Blaschke image points $b(T)$ must lie in the two hyperplanes

$$H_i: \; m_{i,1}u_1 + m_{i,2}u_2 + m_{i,3}u_3 + u_4 - r_i = 0, \quad i = 0, 1, \tag{13}$$

corresponding to the or. spheres C_0, C_1. $H_0 \cap H_1$ is a 2-dimensional plane $f^2 \subset \mathbb{R}^2$. It intersects B in the Blaschke image of Φ. We see that *the Blaschke image of a cone or a cylinder of revolution is an ellipse (planar intersection curve of B).*

The projection of this ellipse onto $u_4 = 0$ is the Gaussian image circle $\gamma(\Phi)$ of Φ; this is a great circle for a cylinder and a small circle for a cone.

Consider hyperplanes H_t in the pencil spanned by H_0 and H_1, represented by an affine combination $(1-t)H_0 + tH_1$ of the two equations in (13). H_t belongs to a sphere with center $(1-t)\mathbf{m}_0 + t\mathbf{m}_1$ and radius $(1-t)r_0 + tr_1$. It is an inscribed sphere of Φ. For $r_0 = r_1$ all inscribed spheres are of equal radius and clearly Φ is a cylinder. Otherwise, one sphere has radius 0. Its t-value is $t_v = r_0/(r_0 - r_1)$, and its center,

$$\mathbf{v} = (1-t_s)\mathbf{m}_0 + t_s\mathbf{m}_1 = \frac{r_1}{r_1 - r_0}\mathbf{m}_0 + \frac{r_0}{r_0 - r_1}\mathbf{m}_1, \tag{14}$$

is the vertex of the cone Φ.

This shows how to find the corresponding surface if one is given a planar cut of B. One passes two general hyperplanes through the plane f^2 and obtains in this way two inscribed spheres.

General cone and cylinder

All tangent planes of a *general cone* Φ pass through its vertex $\mathbf{v}$. Therefore the Blaschke image curve lies in a hyperplane through the origin,

$$p_1u_1 + p_2u_2 + p_3u_3 + u_4 = 0. \tag{15}$$

This hyperplane does not contain the u_4-axis. If Φ is not a right circular cone, it does not have an inscribed sphere with nonvanishing radius and hence $b(\Phi)$ is not planar.

The normal vectors $\mathbf{n}$ of a *general cylinder* Φ are orthogonal to a vector $\mathbf{a}$ in direction of Φ's generating lines, i.e. $\mathbf{a} \cdot \mathbf{n} = 0$. Thus, the points of the curve $b(\Phi)$ lie in the hyperplane

$$a_1u_1 + a_2u_2 + a_3u_3 = 0. \tag{16}$$

This hyperplane contains the u_4-axis. Exactly if Φ is a right circular cylinder, $b(\Phi)$ is planar and, more precisely, an ellipse with center $(0, 0, 0, r)$. Here, r is the radius of Φ.

Other developable surfaces

Any developable surface Φ, different from a plane, has a curve as Blaschke image. If the surface is circumscribed to a sphere of nonvanishing radius, the curve $b(\Phi)$ lies in a hyperplane, which does not pass through the origin,

$$p_1u_1 + p_2u_2 + p_3u_3 + u_4 - c = 0,\ c \neq 0. \tag{17}$$

Let Φ be a developable surface whose tangent planes build a constant angle with a fixed plane $\mathbf{a} \cdot \mathbf{x} + d = 0$ with $\mathbf{a}^2 = 1$. Φ is called *developable surface of constant slope* with respect to $\mathbf{a}$. The unit normal vectors $\mathbf{n}$ of Φ satisfy $\mathbf{n} \cdot \mathbf{a} = c$ where $c \neq 0$ is constant. Thus, the Blaschke image $b(\Phi)$ lies in a fixed hyperplane

$$a_1u_1 + a_2u_2 + a_3u_3 - c = 0,\ c \neq 0. \tag{18}$$

We consider a general developable surface Φ and a fixed tangent plane T, and we compute the osculating plane f^2 of the image curve $b(\Phi)$ at a point $b(T)$ and intersect f^2 with B. The intersection $B \cap f^2$ is an ellipse (13) and it is the Blaschke image of a right circular cone or cylinder $\Gamma(T)$, which has

second order contact with Φ along the ruling of Φ, whose tangent plane is T. Γ is called *osculating cone*.

A curve c on B, which consists of smoothly joined planar pieces $c_1, c_2, \ldots$, can be constructed in a similar way as so-called arc splines on the sphere. The latter consist of smoothly joined planar curve arcs (circular arcs) on the sphere. In fact, the orthogonal projection of c onto $u_4 = 0$ is an arc spline on the Gaussian sphere S^2. By the considerations above, each of the planar segments c_i of c is the Blaschke image $b(\Phi_i)$ of a segment of a right circular cone Φ_i. Therefore, the Blaschke preimage of the entire curve c is a *developable surface composed of smoothly joined right circular cones*. Such *cone spline surfaces* have been studied by S. Leopoldseder [11].

4.2 Surface recognition with principal component analysis on the Blaschke image of estimated tangent planes

Assume that we are given a set of data points $\mathbf{p}_1, \ldots, \mathbf{p}_k \in \mathbb{R}^3$ from a smooth oriented surface Φ. With one of the familiar methods from geometric design we estimate an oriented tangent plane P_i at each data point $\mathbf{p}_i$. Now we would like to check whether the data points come from a surface which is contained in one of the special classes discussed above.

The surface recognition procedure uses the Blaschke image points $\mathbf{b}_i = b(P_i) \in \mathbb{R}^4$ of the planes P_i. We check if the point cloud $\mathbf{b}_0, \ldots, \mathbf{b}_k$ on B can be fitted well by a hyperplane H. To achieve this, we perform a *principal component analysis* on the image points $\mathbf{b}_1, \ldots, \mathbf{b}_k$. This is equivalent to fitting the data point cloud $\mathbf{b}_1, \ldots, \mathbf{b}_k$ by a hyperplane, which minimizes the sum of squared Euclidean distances in $\mathbb{R}^4$. The unknown hyperplane is written in the Hesse normal form as

$$H: \; h_0 + h_1 u_1 + \ldots + h_4 u_4 = 0, \quad h_1^2 + \ldots + h_4^2 = 1. \tag{19}$$

The signed Euclidean distance $d(\mathbf{b}_i, H)$ is now

$$d(\mathbf{b}_i, H) = h_0 + h_1 b_{i,1} + \ldots + h_4 b_{i,4} = h_0 + \mathbf{h} \cdot \mathbf{b}_i, \tag{20}$$

where $\mathbf{h} = (h_1, \ldots, h_4)$ denotes the unit normal vector of H. The minimization of the sum of squared distances,

$$F_2(h_0, h_1, h_2, h_3, h_4) \;=\; \frac{1}{k} \sum_{i=1}^{k} d^2(\mathbf{b}_i, H)$$

$$= \frac{1}{k}\sum_{i=1}^{k}(h_0 + \mathbf{b}_i \cdot \mathbf{h}_i)^2, \tag{21}$$

is the minimization of the quadratic form F_2 in the unknowns $h_0, \ldots, h_4$ under the quadratic constraint $\mathbf{h}^2 = 1$. This is a general eigenvalue problem with a quartic characteristic equation.

It is well-known and easy to see that the regression hyperplane H passes through the barycenter $\mathbf{c} = (\sum \mathbf{b}_i)/k$ of the k data points $\mathbf{b}_i$. Using $\mathbf{c}$ as new origin, the coordinate vectors of the data points become $\mathbf{q}_i = \mathbf{b}_i - \mathbf{c}$ and the unknown hyperplane H has vanishing coefficient, $h_0 = 0$. F_2 is now written as

$$F_2(h_1, h_2, h_3, h_4) = \frac{1}{k}\sum_{i=1}^{k}(\mathbf{q}_i \cdot \mathbf{h}_i)^2. \tag{22}$$

It is a quadratic form in the unknowns $h_1, \ldots, h_4$. Using a matrix notation with vectors as columns, it is written as

$$F_2(\mathbf{h}) = \mathbf{h}^T \cdot C \cdot \mathbf{h}, \quad \text{with } C := \frac{1}{k}\sum_{i=1}^{k} \mathbf{q}_i \cdot \mathbf{q}_i^T. \tag{23}$$

The symmetric matrix C is known as covariance matrix in statistics and as inertia tensor in mechanics. Minimizing F_2 under the constraint $\mathbf{h}^2 = 1$ is an ordinary eigenvalue problem. Let λ_i be an eigenvalue of C and let $\mathbf{h}_i$ be a corresponding normalized eigenvector ($\mathbf{h}_i^2 = 1$). Then, $\lambda_i = F_2(\mathbf{h}_i)$. Therefore, the best fitting hyperplane H_1 belongs to the smallest eigenvalue λ_1. The statistical standard deviation of the fit with H_1 is

$$\sigma_1 = \sqrt{\lambda_1/(k-4)}. \tag{24}$$

The *distribution of the eigenvalues* $\lambda_1 \leq \lambda_2 \leq \cdots \leq \lambda_4$ of the covariance matrix C (and the corresponding standard deviations $\sigma_1 \leq \cdots \leq \sigma_4$) gives important information on the shape of the surface Φ:

- Assume that there is a single small eigenvalue λ_1 (small standard deviation σ_1). The corresponding well fitting hyperplane $H_1 : h_{1,0} + \ldots h_{1,4}u_4 = 0$ characterizes a sphere C_1 in $\mathbb{R}^3$, whose center $\mathbf{m}_1$ and radius r_1 are computed as

$$\mathbf{m}_1 = \frac{1}{h_{1,4}}(h_{1,1}, h_{1,2}, h_{1,3}),\ r_1 = -\frac{h_{1,0}}{h_{1,4}}. \tag{25}$$

Then, we check, whether the points $\mathbf{b}_i$ form a curve-like or a surface-like arrangement on B (see section 5). If the arrangement of points $\mathbf{b}_i$ is surface-like, then the surface Φ is close to the *sphere* C_1. A curve-like arrangement characterizes a developable surface Φ, which is tangent to a sphere (close to C_1), compare (17). A small radius r_1 of C_1 indicates the presence of a *cone* (not a rotational one), compare (15).

So far, we have tacitly assumed $h_{1,4} \neq 0$. Vanishing $h_{1,4}$ characterizes a *developable surface of constant slope*, compare (18). If additionally $h_{1,0} = 0$, the surface Φ is a *general cylinder*, compare (16). Also a small value of $h_{1,4}$, which gives rise to a center $\mathbf{m}_1$ which is far away from the considered object, indicates the presence of a cylinder.

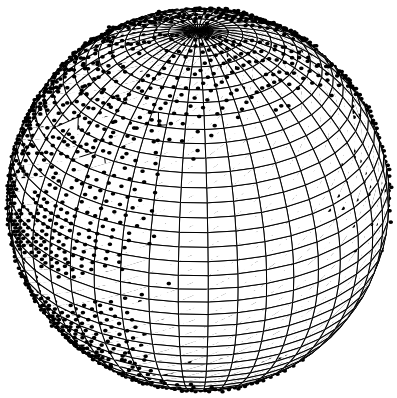

Figure 3: Data points of a tennis-ball and reconstructed object.

Figure 3 shows a point cloud obtained from scanning a tennis-ball and the reconstructed object. The eigenvalues with respect to the minimization of (22) are

$$\lambda_1 = 0.00004,\ \lambda_2 = 0.18820,\ \lambda_3 = 0.35731,\ \lambda_4 = 0.37100,$$

and shows one small eigenvalue which leads to one hyperplane H containing the Blaschke image of the estimated tangent planes. The estimated radius of the sphere is 0.9928, since before computing the data

are uniformly scaled. The mean distance between the data points and the estimated center is 0.994 which nearly equals the estimated radius.

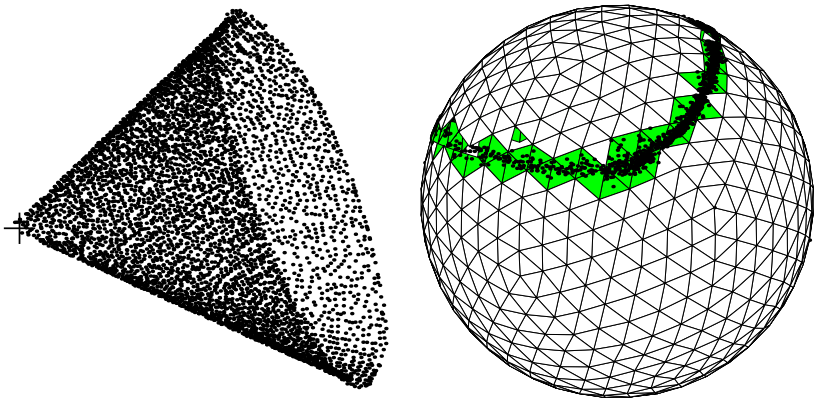

Figure 4: Left: Data points of a general quadratic cone and estimated vertex, indicated by a cross. Right: Blaschke image, orthogonally projected onto S^2.

Figure 4 shows a point cloud obtained from scanning a general quadratic cone without rotational symmetry. Outliers of the Blaschke image have been removed by *morphological cleaning* and removing cells which carry only a view points, compare section 5.1. The eigenvalues according to the minimization of (22) are

$$\lambda_1 = 0.00433,\ \lambda_2 = 0.01480,\ \lambda_3 = 0.17442,\ \lambda_4 = 0.57563,$$

and shows one small eigenvalue which leads to one hyperplane H containing the Blaschke image of the estimated tangent planes. The estimated 'radius' (according to (25)) is $r = 0.0041$. This tells us that the estimated tangent planes shall pass through a fixed point. The analysis of the dimension of the Blaschke image shows that it is curve-like.

- If there are two small eigenvalues and corresponding standard deviations $\sigma_1 \leq \sigma_2$, we get two well fitting hyperplanes H_1, H_2. Center and radius of C_2 follow analogously to (25). In fact, we have a pencil of well-fitting hyperplanes, showing that the 2-dimensional plane $H_1 \cap H_2$

fits the data points $\mathbf{b}_i$ well. From the discussion in section 4.1, we know that this reveals the surface Φ as *right circular cone or right circular cylinder*. It possesses two inscribed spheres C_1 and C_2. The axis of the surface is spanned by their centers $\mathbf{m}_1, \mathbf{m}_2$. Nearly equal radii characterize a cylinder. Otherwise, we have a cone and compute an estimate of its vertex according to (14).

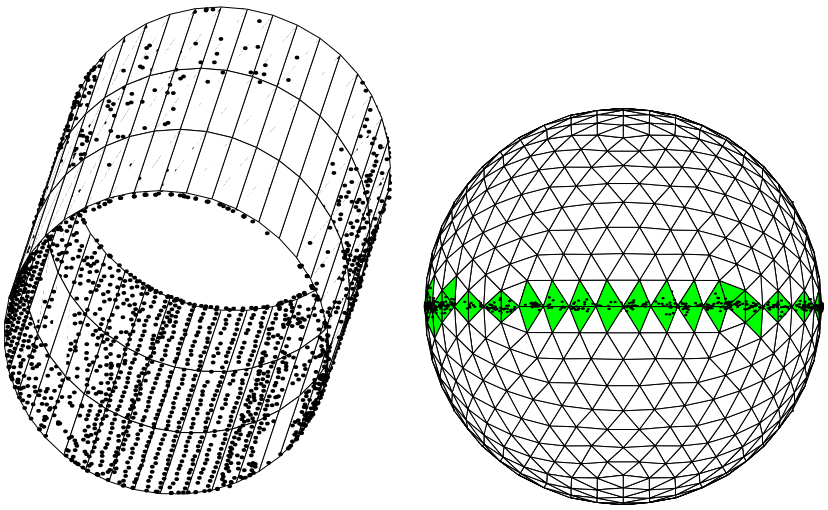

Figure 5: Left: Data points of a cylinder of revolution and reconstructed object. Right: Blaschke image (cleaned and resampled), orthogonally projected onto S^2.

Figure 5 shows a point cloud obtained from scanning a cylinder of revolution and the reconstructed object. Outliers in the Blaschke image have been removed by *cleaning* and removing cells which carry only a view points. The eigenvalues according to the minimization of (22) is

$$\lambda_1 = 0.00013,\ \lambda_2 = 0.00023,\ \lambda_3 = 0.48055,\ \lambda_4 = 0.51496,$$

and shows two small eigenvalues which lead to two hyperplanes H_1, H_2 containing the Blaschke image of the estimated tangent planes. The estimated radii of the spheres determined by H_1, H_2 are $r_1 = 0.6707, r_2 =$

0.6636. This indicates that the original surface has been a right circular cylinder.

- It is impossible that there are exactly three small eigenvalues, since this indicates that the data points $\mathbf{b}_i$ on the Blaschke cylinder are nearly collinear. Then they need to be close to a ruling of the cylinder, which means that the tangent planes of Φ are nearly parallel to each other. This happens only, if the surface Φ is close to a *plane*. Then, however, we have four small eigenvalues, and a point-like cluster of data points $\mathbf{b}_i$ on B, see Figures 8 and 9.

There are several issues which need to be addressed in a successful implementation of the method.

- In all cases, the size of σ has to be judged in comparison to the size of the object to be investigated.

- The methods presented above are able to compute an estimate for an approximating plane, sphere, cone or cylinder of revolution. Also the vertex of a general cone or the directions of the rulings of a general cylinder can be computed. In all these cases, one will use these approximants for *segmentation of the data* and – if necessary – as an initial fit. Knowing the surface type, the final fit should be performed by a method working directly on the relevant data points $\mathbf{p}_i$ (see details and references in the survey by Varady and Martin [28]).

- A curve-like arrangement of data points $\mathbf{b}_i$ on the Blaschke-cylinder indicates a developable surface. In the general case, it will not have an inscribed sphere. We can fit the data points on B by a curve $\mathbf{c}(t) \subset B$. In $\mathbb{R}^3$, this gives a one-parameter family of planes, whose envelope is an approximating developable surface. This procedure seems to be simpler than it is. The major problem with general developable surfaces Φ is their singular curve c_s (the surface Φ is formed by the tangents of this curve). In applications, one wants to have c_s outside the area of interest. Pushing away the singular curve from the area of interest can also be done in the Blaschke model: the osculating plane at a curve point $\mathbf{c}(t)$ intersects B in an ellipse, which is the Blaschke image of the osculating cone. The vertex of this cone is a point of c_s. It would lead too far to elaborate this here in more detail and thus we defer this topic

to another publication. We just mention two previous publications on this topic, which work with cone spline surfaces [3, 11] and special rational developable surfaces [19], respectively.

- In the theoretical formulation given above, we use simple least squares methods. These are sensitive to outliers. In practical applications, one uses more robust schemes. One way is to minimize a weighted sum of squared distances $F = \sum w_i d^2(\mathbf{b}_i, H)$ within a weight iteration. Appropriate weighting schemes are found in the literature on robust regression [23]. Some outliers are eliminated efficiently by a morphological cleaning operation as discussed in section 5.1. A further alternative would be to use the RANSAC principle, which enjoys great popularity in Computer Vision [6]. There are also contributions on robust principal component analysis [5].

- A real object will have faces which belong to different classes of surfaces. The proposed methods are then not applied to the whole set of estimated tangent planes. One first recognizes edges on the objects and splits the data set there. Moreover, one uses the proposed surface recognition procedures, implemented in a robust way, as local filters. They are applied to sufficiently large neighborhoods of data points and those are then characterized as belonging to a certain class of surfaces (plane, sphere, cone, cylinder, ...). One could say that this results in an 'image' defined on a triangular mesh. The mesh has as vertices the data points $\mathbf{p}_1, \ldots, \mathbf{p}_k$ and its faces carry a label (0,1,2,...) according to the locally detected surface type. Processing such labeled images (or binary images in the case of just 2 values) on meshes can be done by techniques from *mathematical morphology*. This will be briefly indicated in section 5.1 and shall be pursued in more depth in future research.

5 Implementation and examples

5.1 Processing the Blaschke image with mathematical morphology

We consider a triangular mesh Δ in $\mathbb{R}^3$, whose vertices are the given data points $\mathbf{p}_1, \ldots, \mathbf{p}_k$. One may view the methods described above as filters,

which assign to each triangle in the data mesh Δ a probability p, with which it lies in a region of a certain surface type. If we fix the type, say spherical, and set a threshold on p, we get a *binary image on the mesh* Δ: a black face indicates membership to a spherical region, and a white face does not. We may have different spheres or different surfaces types. Then we get a *labeled image*, where to each face we assign values from a small set V. Finally, we could even use probabilities or other indicators with values in some interval (discretely resolved). This would represent a *greylevel image on the mesh*. In all cases, it is very desirable to have processing tools for those auxiliary images on a mesh. The mesh could also be on the Gaussian sphere. We have discussed a discretization of the Blaschke cylinder and it is also very helpful to consider such images defined on the cells of the discretized Blaschke cylinder.

Image processing frequently uses *mathematical morphology* for basic topological and geometric operations [7, 24, 25]. Just a few contributions [8, 12, 21, 22, 29] extend morphology to curved manifolds and to meshes and cell decompositions on curved manifolds, such as the Blaschke cylinder. Based on this work, we have started to extend it and to use it in the present context. Let us briefly describe this here.

A basic element of mathematical morphology on binary images is the definition of a *structuring element* Σ. Minkowski sums between Σ and the considered white or black parts of the image are used for the definition of *dilation* and *erosion*. These are discrete versions of (generalized) offsetting operations. Dilation and erosion are basic building blocks of more powerful operations such as *opening* or *closing*. The Minkowski sum requires the availability of translations which move the structuring element to the desired places of the image. This is exactly the point where curved manifolds create problems. There is no really useful translation on it, since the geodesic translation known in differential geometry is path dependent in case of non-vanishing Gaussian curvature [21, 22]. One way to overcome this is the use of approximants to *geodesic circles* as local neighborhoods (positions of the structuring element). Another way is to define such local neighborhoods in a purely topological way. In this case we can base the considerations upon *morphology on graphs* [8, 12, 29].

We split the discussion into two parts. At first we discuss local neighborhoods, to be understood as positions of the structuring element. Secondly, we show how to use the neighborhoods – independently from their creation – in the formulation of morphological operators. In both cases we confine

ourselves to triangular meshes.The mesh is called Δ, but it needs not be the one to the data points. An extension to other cell arrangements, like those in the discretized Blaschke cylinder, proceeds along similar lines.

Neighborhoods

The *purely topological neighborhood* $N_1(\Delta_i)$ of *depth one* to a triangle Δ_i consists of all triangles in Δ, which share at least one vertex with Δ_i. The neighborhood N_k is defined by iterating the procedure: in step k we add all triangles which share at least one vertex with the boundary of N_{k-1}.

For a nearly uniform triangulation, the neighborhoods N_k are good approximants to geodesic circles. Otherwise, one may use a further *geometric criterion* to restrict the choice of triangles in N_k. For example, a triangle is only added to N_k if the spatial (or the geodesic) distance of its barycenter to the barycenter of Δ_i is below a prescribed threshold. We have also experimented with a distance definition between triangles, which includes spatial distance between their centers and the angle between their normals. The shapes of such neighborhoods are elongated in direction of smaller normal curvatures, a very useful effect for the processing of edges.

Morphological Operators

Let us first describe the *dilation* of level k of black parts (object P) on a white background. At each boundary triangle Δ_i of P (which may have many connected components) we compute the local neighborhood $N_k(\Delta_i)$ and color it black. Under certain assumptions, one may be able to prove the following counterpart to the planar case: performing k times a dilation of level one is the same as performing once a dilation of level k. For geodesic offsets this would be true. Roughly speaking, a dilation is a discrete offsetting operation.

An *erosion* of level k of black parts is just a dilation of level k applied to the white background. From now on, all operations are viewed as being applied to the object (black part of the image).

A morphological *closing* operation first applies a dilation of level k, and then an erosion of level k. This fills holes.

The *opening* operator applies the erosion before the dilation, which removes thin connections between more compact parts. The width of such bridges to be removed has to be in accordance to the depth k.

The *thinning* operator of depth k inspects the boundary of P. It removes those boundary triangles Δ_i, which have just one black component in $N_1(\Delta_i)$. This can be iteratively applied (or one works with neighborhoods of depth k). Note that this operation does not remove bridges: those give rise to at least two components in $N_1(\Delta_i)$.

Finally, *cleaning* an image is extremely useful for outlier elimination in our techniques. It eliminates those black triangles Δ_i, which are the only black ones in $N_k(\Delta_i)$.

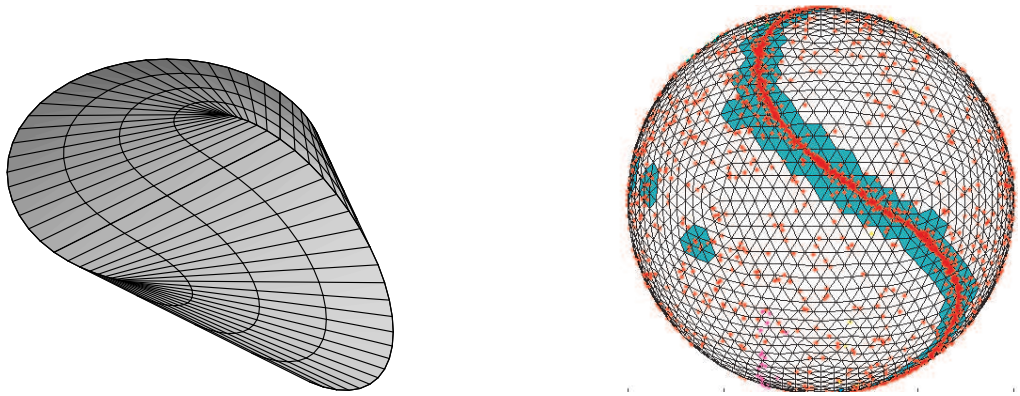

Figure 6: Left: Cad-model of a developable surface. Right: Blaschke image of a developable, projected onto the Gaussian sphere S^2.

Figures 6 and 7 show morphological operations applied to the Blaschke image of the estimated tangent planes of the developable surface. Since it is hard to imagine the generating lines of this surface from a figure showing data points, Figure 6 shows a cad-model instead.

5.2 Examples

We like to present two further examples for the recognition of special geometric parts in an object. The objects of the previous examples in section 4.2 and the first object which will be described here have been scanned with a laser scanner (Minolta VI-900) from different sides and the different scans have been merged (registration). Using commercial software, a triangulation of the point cloud has been computed. Most of the algorithms described here are implemented in Matlab and C.

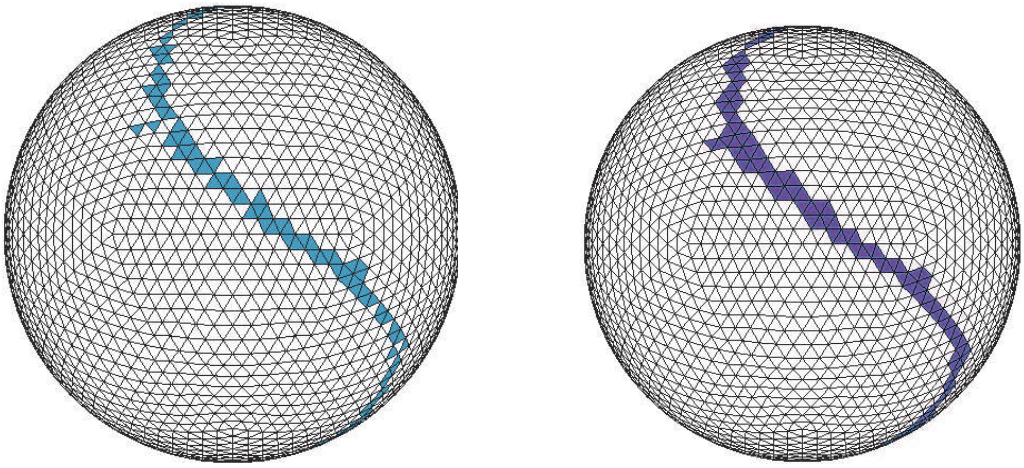

Figure 7: Left: Cleaning of the Blaschke image. Right: Closing of the Blaschke image.

Fig. 8 shows the first object which is composed of planar pieces only. The detected edges of the object are represented by black triangles. The computation of the hyperplanes of regression for the two largest segmented regions R_i shows the following eigenvalues. This indicates that the Blaschke images $b(R_i)$ are point-like cluster in B.

$$\begin{aligned} R_1: &\quad 0.00001, 0.00018, 0.00175, 0.00315 \\ R_2: &\quad 0.00001, 0.00046, 0.00112, 0.00201 \end{aligned}$$

Fig. 9 shows the second object which consists of planes, cylinders, cones of revolution and spherical parts. The data points are generated artificially by sampling a mathematical model. After having computed the edges and the Blaschke image of the object, the dimension of the Blaschke image has been analyzed. It is possible to recognize cylindrical and conical parts and finally the spherical part of the object. The computation of the hyperplanes of regression to the parts of the object gives the following eigenvalues:

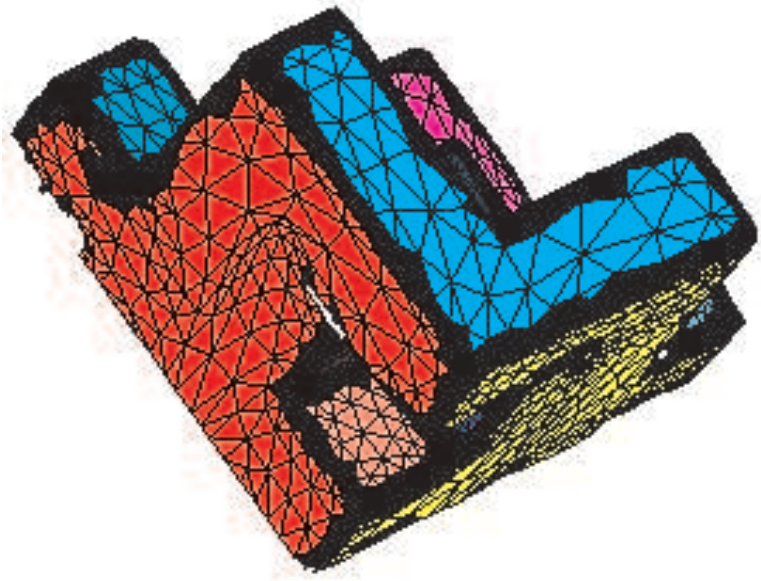

Figure 8: Segmentation of a piecewise planar object.

Planar vertical region left:
eigenvalues: 0.00000, 0.00006, 0.00098, 0.00200.
Cylinder of rotation, front:
eigenvalues: 0.00002, 0.00069, 0.10908, 0.62807.
Cone of rotation:
eigenvalues: 0.00001, 0.00079, 0.36814, 0.55629.
Spherical part:
eigenvalues: 0.00000, 0.07370, 0.33614, 0.51365.

6 Conclusion and Future Research

We have shown how the classical geometric Blaschke model of Laguerre geometry is related to the Hough transform and how it can be used to detect special shapes in point clouds. Moreover, we have presented initial results on the use of mathematical morphology on meshes in processing tasks which appear in the context of automatic shape understanding and reconstruction.

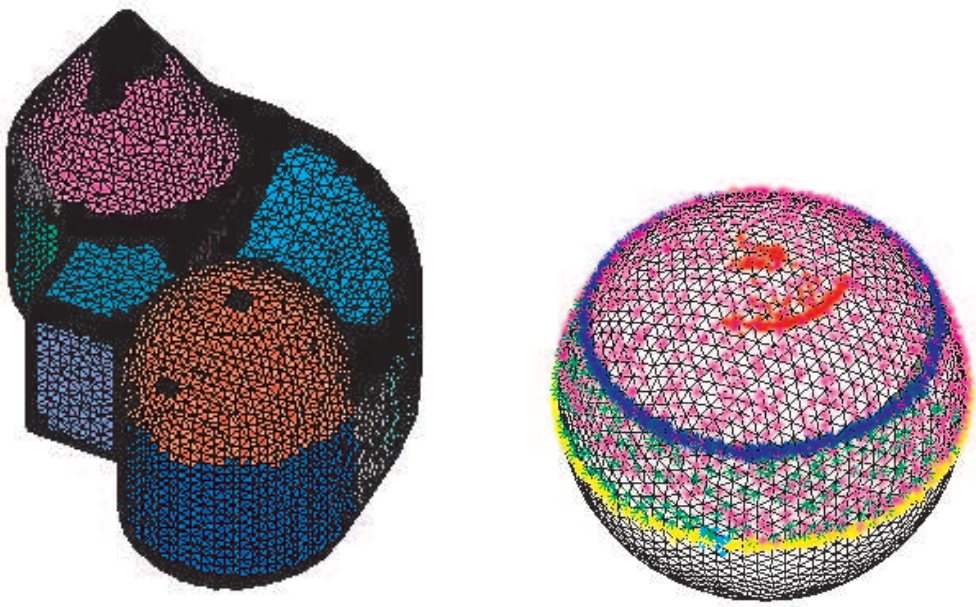

Figure 9: Left: Segmentation of an object which consists of planar, cylindrical, conical and spherical parts. Right: Blaschke image projected onto S^2.

There are many directions for future research, including the following ones.

- Mathematical morphology on meshes and discrete representations of higher-dimensional curved manifolds needs more research. Fundamental research, implementation issues and applications are of interest here. Moreover, we need to work on greylevel images as well.

- Another interesting topic is a study of the *distortions* in the mapping between Φ and $b(\Phi)$, or between their discrete representations Δ and $\bar{\Delta}$. Obviously, both developable surfaces and highly curved regions give rise to heavy distortions. These distortions may be seen as functions (greylevel images) on the meshes Δ or $\bar{\Delta}$. Mathematical morphology on those images can aid the segmentation task.

- Differential geometric invariants of Laguerre geometry or invariants of appropriate subgroups of the Laguerre group would also deserve an investigation with respect to their use in segmentation tasks.

Acknowledgements

This work has been funded by the Austrian Science Fund through grant P16002-N05 and by the innovative project "3D Technology" of Vienna University of Technology. We would like to thank Allan Hanbury for stimulating discussions on mathematical morphology and Michael Hofer for his help with data acquisition and valuable comments on an earlier version of this paper.

References

[1] W. Benz, *Geometrische Transformationen*, BI-Wiss. Verlag, Mannheim (1992).

[2] W. Blaschke, Untersuchungen über die Geometrie der Speere in der Euklidischen Ebene. *Monatshefte für Mathematik und Physik* **21**, pp. 3–60 (1910).

[3] H.-Y. Chen, I.-K. Lee, S. Leopoldseder, H. Pottmann, T. Randrup, J. Wallner, On surface approximation using developable surfaces, *Graphical Models and Image Processing* **61**, pp. 110–124 (1999).

[4] J. L. Coolidge, *A Treatise on the Circle and the Sphere*, Clarendon Press, Oxford (1916).

[5] F. De la Torre and M. J. Black, Robust principal component analysis for Computer Vision, *Proc. 8th Int. Conf. on Computer Vision*, pp. 362–369 (2001).

[6] R. Hartley, A. Zisserman, *Multiple View Geometry in Computer Vision*, Cambridge Univ. Press, Cambridge, UK (2000).

[7] H. J. A. M. Heijmans, *Morphological Image Operators*, Academic Press, Boston (1994).

[8] H. J. A. M. Heijmans, P. Nacken, A. Toet, L. Vincent, Graph Morphology, *Journal of Visual Communication and Image Representation* **3**, pp. 24–38 (1992).

[9] J. Illingworth, J. Kittler, A survey of the Hough transform, *Computer Vision, Graphics and Image Processing* **44**, pp. 87–116 (1988).

[10] V. F. Leavers, Which Hough transform? *CVGIP: Image Understanding* **58**, pp. 250–264 (1993).

[11] S. Leopoldseder, Cone spline surfaces and spatial arc splines – a sphere geometric approach, *Advances in Computational Mathematics* **17**, pp. 49–66 (2002).

[12] N. Loménie, L. Gallo, N. Cambou, G. Stamon, Morphological operations on Delauney triangulations, *Proc. Intl. Conf. on Pattern Recognition*, ICPR'00-Vol.3, (2000).

[13] Y. Muller, R. Mohr, Planes and quadrics detection using Hough transform, *Proc. 7th Intl. Conf. on Pattern Recognition*, Montreal, pp. 1101-1103 (July 1984).

[14] N. Navab, Canonical representation and three view geometry of cylinders, *Intl. Archives of the Photogrammetry, Remote Sensing and Spatial Information Sciences*, Commission III, Vol. XXXIV, Part 3A, pp. 218–224 (2002).

[15] N. M. Patrikalakis, T. Maekawa, *Shape Interrogation for Computer Aided Design and Manufacturing*, Springer (2002).

[16] M. Peternell, H. Pottmann, Approximation in the space of planes – Applications to geometric modeling and reverse engineering, *Revista de la Real Academia de Ciencias, Serie A: Matematicas* **96** (2), pp. 243–256 (2002).

[17] H. Pottmann, S. Leopoldseder, Geometries for CAGD, in: *Handbook of Computer Aided Geometric Design*, G. Farin, J. Hoschek and M.S. Kim, eds, North Holland, pp. 43–73 (2002).

[18] H. Pottmann, M. Peternell, Applications of Laguerre geometry in CAGD, *Computer Aided Geometric Design* **15**, pp. 165–186 (1998).

[19] H. Pottmann, J. Wallner, Approximation algorithms for developable surfaces, *Computer Aided Geometric Design* **16**, pp. 539–556 (1999).

[20] H. Pottmann, J. Wallner, *Computational Line Geometry*, Springer-Verlag (2001).

[21] J. B. T. M. Roerdink, Mathematical morphology on the sphere, *Proc. SPIE Conf. Visual Communications and Image Processing '90*, Lausanne, pp. 263–271 (1990).

[22] J. B. T. M. Roerdink, Manifold Shape: from Differential Geometry to Mathematical Morphology, in: *Shape in Picture*, Y.L. O et al, eds., Springer, Berlin, pp. 209–223 (1994).

[23] P. J. Rousseeuw, A. M. Leroy, *Robust Regression and Outlier Detection*, Wiley, New York (1987).

[24] J. Serra, *Image Analysis and Mathematical Morphology*, Academic Press, London (1982).

[25] J. Serra, ed., *Image Analysis and Mathematical Morphology, Vol. 2: Theoretical Advances*, Academic Press, London (1988).

[26] J. Vanden Wyngaerd, L. Van Gool, R. Koch, M. Proesmans, Invariant based registration of surface patches, *Proc. Intl. Conference on Computer Vision*, Kerkyra, Greece, pp. 301–306 (1999).

[27] T. Várady, P. Benkö and G. Kós, Reverse engineering regular objects: simple segmentation and surface fitting procedures, *Int. J. Shape Modeling* **4**, pp. 127–141 (1998).

[28] T. Várady, R. Martin, Reverse Engineering, in: *Handbook of Computer Aided Geometric Design*, G. Farin, J. Hoschek and M.S. Kim, eds., North Holland, pp. 651–681 (2002).

[29] L. Vincent, Graphs and mathematical morphology, *Signal Processing* **16**, pp. 365–388 (1989).

[30] G. Vosselman, S. Dijkman, 3D building model reconstruction from point clouds and ground plans, *Intl. Archives of Photogrammetry and Remote Sensing*, Vol. XXXIV-3/W4, Annapolis, MD, pp. 37–43 (2001).